Chapter 8
Optimized Test Design for Identification of the Variation of Elastic Stiffness Properties of Loblolly Pine (*Pinus taeda*) Pith to Bark

D.E. Kretschmann, J.M. Considine, and F. Pierron

Abstract This article presents the design optimization of an un-notched Iosipescu test specimen whose goal is the characterization of the material elastic stiffnesses of a Loblolly (*Pinus taeda*) or Lodgepole pine (*Pinus contorta*) sample in one single test. A series of finite element (FE) and grid simulations were conducted to determine displacement and strain fields for various ring angles, ring spaces, and proportions of latewood per ring. These displacement and strain fields were utilized to determine the constitutive parameters for the woody material using VFM. Using an error function based on a comparison of the input stiffnesses and those identified by grid simulation information it was possible to narrow the optimum ring angle at which test specimens should be tested. The results of this work suggest that the starting angles for the un-notched Iosipescu test specimens should be approximately 45° to produce the smallest identification error.

Keywords Experimental design • Un-notched Iosipescu test • Virtual fields method (VFM) • Elastic stiffness parameters • Computer simulations

8.1 Introduction

Dramatic differences in properties can be observed in juvenile material, which grows close to the pith of a tree, versus the more mature material that grows near the bark of a tree [1]. Development of techniques to more easily understand the variation of mechanical properties for wood from pith to bark is needed. This information can be used to help explain the large variation in properties and dimensional stability of solid wood products observed when cut from different positions within the tree. Virtual Fields Method (VFM) has proven to be an appropriate technique to determine local, heterogeneous constitutive properties [2]. Xavier and others have demonstrated the possibility of using a VFM to determine the transverse and shear properties of wood in a tree [3, 4]. Work is underway to develop testing procedure that uses VFM as a method of documenting the natural variations in longitudinal, transverse, and shear stiffnesses that occur in Loblolly and Lodgepole pine both within a tree and between trees.

In the portion of the study being reported here, a procedure has been developed to simulate the un-notched Iosipescu test using a finite element (FE) model and a simulated grid pattern to create synthetic displacements and strains. Using this information the VFM was applied to subsequently extract all the earlywood and latewood stiffness parameters for both the FE model and the grid simulation. The uncertainty of the grid measurement, including the systematic and random errors, will be evaluated thoroughly by including several different sources of error. This paper directly reports on one portion of the systematic error. An optimization study was undertaken to look at the impact of ring angle, ring spacing and proportion of earlywood and latewood, and anisotropy ratios (position in tree). This work was conducted to facilitate the selection of ring angle for material property determination. By minimizing the value of an error function at different conditions a range of optimal ring angles for the test configuration was determined.

D.E. Kretschmann (✉) • J.M. Considine
USDA Forest Service, Forest Products Laboratory, One Gifford Pinchot Drive, Madison, WI 53726, USA
e-mail: dkretschmann@fs.fed.us

F. Pierron
University of Southampton, Southampton SO17 1BJ, UK

C. Sciammarella et al. (eds.), *Experimental and Applied Mechanics, Volume 4*,
Conference Proceedings of the Society for Experimental Mechanics Series, DOI 10.1007/978-3-319-22449-7_8

8.2 Methods

8.2.1 Background on Loblolly and Lodgepole Pine Study Material

A study is underway that examines the variation of Loblolly and Lodgepole pine properties from different growth conditions in the South and Western part of the United States [5–8]. The Loblolly pine trees were harvested from two different locations in the state of Arkansas and the Lodgepole pine trees are from four different sites in the U.S. Intermountain West. The western trees included site variations affecting growth, such as elevation, precipitation, and growing seasons. Bolts were extracted from each tree and processed to extract a single, radial-sawn board from each bolt (Fig. 8.1a).

As many 80 × 20 × 5 mm specimens oriented with the growth ring grain pattern, at an angle yet to be determined, will be cut from each board. Variation in the width from pith to bark will result in different number of samples being taken from the North (N) or South (S) side of the board (Fig. 8.1b). For each specimen tree number, sample number, position (N or S) and the ring number from the center of the specimen will be recorded. This information will be used to assess the impacts of position within and between trees.

8.2.2 Experimental Test Methods

Testing will be conducted on an Instron universal test frame configured to run an Iosipescu test with the specimens having the V-notches removed from the classical geometry (Fig. 8.2, un-notched test). It has been shown that a complex and heterogeneous strain field is generated across the central part (L × W Fig. 8.1c) of the Iosipescu test specimen [2]. For these tests the load will be applied at a controlled displacement rate of 1 mm per minute and measured with a 100 kN load cell. The tests will be stopped at approximately 400 N so that the specimen remains in the linear elastic regime. These tests will be carried out at room temperature 23 ± 1 °C and at a relative humidity of 50 ± 2 %. For each sample oven dry density will be determined.

8.2.3 Parameter Identification from Virtual Fields Method

In order to apply the VFM technique full-field displacements measurements must be obtained and the equations for virtual work used to determine the various constitutive parameters of a material. The full-field displacements will be determined using a grid method and digital photography.

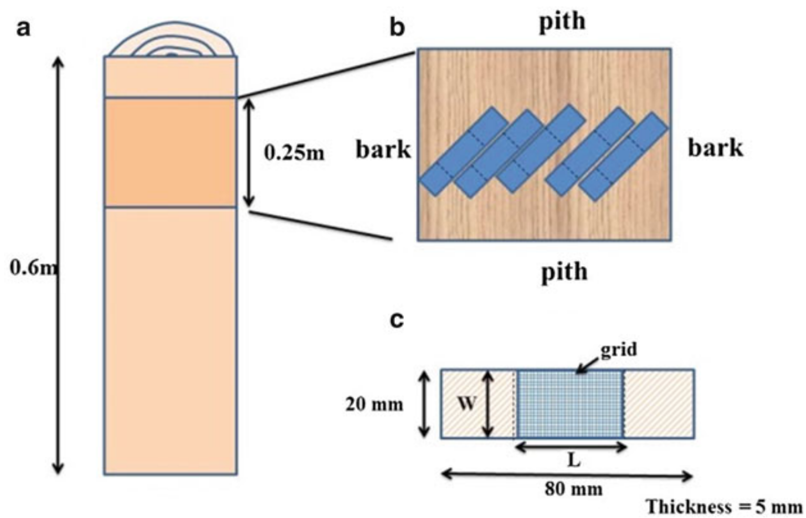

Fig. 8.1 Material sampling: (**a**) log; (**b**) pith to bark test sample cut out pattern; (**c**) dimensions of test specimen

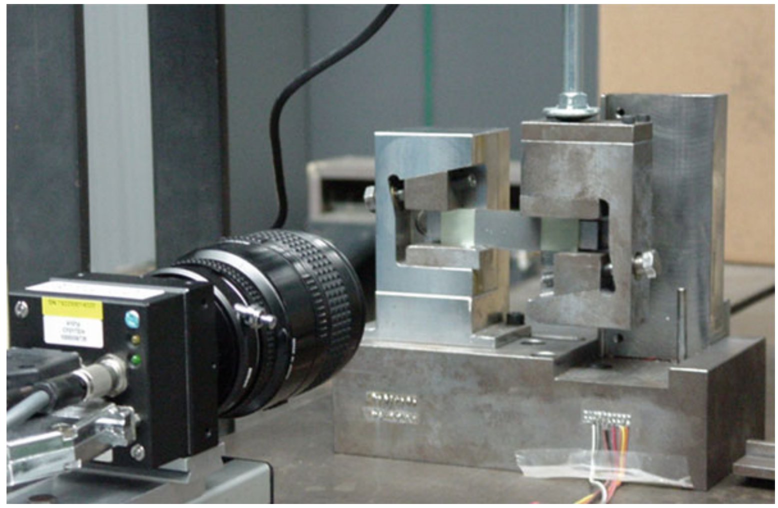

Fig. 8.2 Example of an Un-notched Iosipescu test fixture [9]

8.2.4 Full-Field Displacements Measurement Technique

The grid method measures in-plane full-field displacements by analyzing the deformation of a grid pattern of orthogonal light and dark lines which have been captured by a digital camera. To determine a continuous function that predicts the full-field displacement a series of before and after digital images of the grid pattern are analyzed to determine a polynomial function that fits the deformation pattern observed. Using a spatial phase-shifting method for a given image of the grid a phase function for each image can be evaluated [10]. A phase map can be developed for the image. The difference in phase maps before and after loading is proportional to the displacement field. By using before and after recorded images and the corresponding phase fields the full field displacements can be determined. An additional step is required to calculate the corresponding strain field. Using a least-squares approximations a fit of a two dimensional polynomial function to the raw displacement data is conducted. For previous VFM work with wood a seventh degree polynomial function was found suitable for the least-squares regression scheme [3]. Since the aim of this technique is to identify all the material properties in one single test, the experiment should be designed to induce balanced heterogeneous strain maps so all the components can be identified. A series of simulations have been conducted to select the optimal orientation of the Iosipescu specimen to achieve balanced strain maps.

8.3 Finite Element and Grid Simulations

Three steps are required to determine what ring angle might produce an acceptable balanced heterogeneous strain map: (1) Construction of a FE model that mimics the loading configuration of the un-notched Iosipescu test that provides a numerically-modeled displacement field; (2) Using the FE displacement field as input to a grid simulator [11] grid displacements and strains, based on camera parameters, are created; and (3) Use the constitutive properties identified by VFM for the FE model (no noise numerical data) and the grid simulation (experimentally-simulated data) to determine an optimal ring angle based on evaluation of an error function which minimizes the systematic error between constitutive components.

8.3.1 Finite Element Model

The FE analysis to simulate the un-notched Iosipescu specimen was performed using ANSYS® (ANSYS, Inc., Canonsburg, PA 15317, USA). The dimensions of the model are shown in Fig. 8.3. The model used 608,000 square elements with 400 elements per mm^2 or 20 nodes per millimeter. There were 240,000 square elements in the active area of the model (20 by

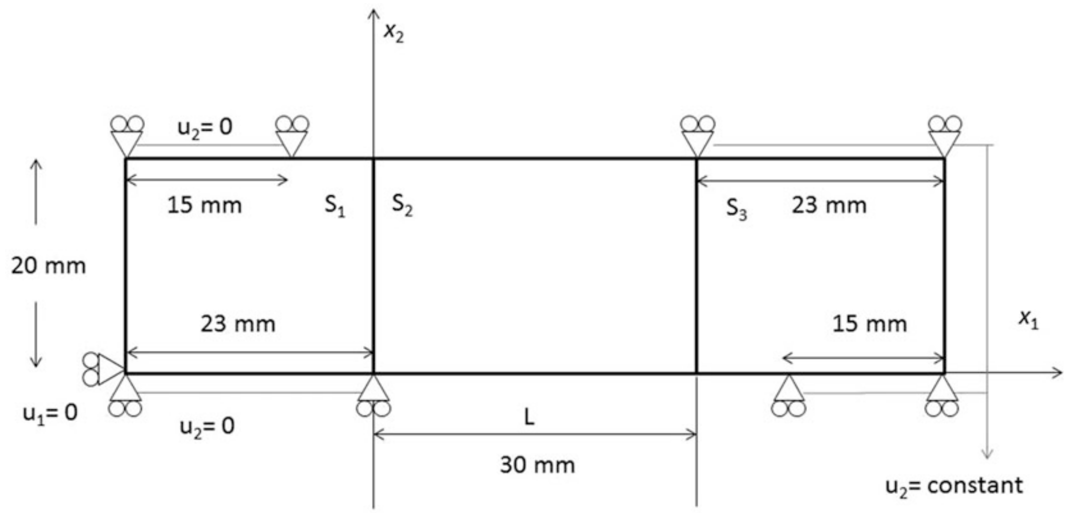

Fig. 8.3 Dimensions of the Iosipescu FE specimen

30 mm sample portion with grid). A 400 N force was applied to the model which was selected based on earlier experimental measurements of the material so that the behavior would remain elastic. The material properties for Loblolly pine were used for these simulations.

8.3.2 *Material Property Input for FE Modeling*

Our selection of property inputs has been based information on obtained through testing of Loblolly pine (*Pinus taeda*) that occurred during 2004 through 2010 [5–7]. The earlywood and latewood Loblolly pine data was gathered on two trips to Loblolly pine plantations in Arkansas. Recommended E_L, E_T, and G values were arrived at after looking at all of this information. It was decided that an appropriate approximation of E_L is 0.60×10^6 (4.14 GPa) and 1.65×10^6 psi (11.38 GPa) for earlywood and latewood respectively. A ratio of E_L to E_T could be taken as 27 for earlywood and of 13 for latewood. Finally, a value of G of 0.11×10^6 psi (0.76 GPa) and 0.25×10^6 psi (1.72 GPa) for earlywood and latewood respectively should be appropriate. It has been shown that latewood closer to the pith is similar in properties to earlywood [5, 6]. As a first approximation of the properties of latewood close to the pith, the latewood properties shown above were cut in half when the simulations were run to mimic material near the pith. Poison's Ratio for all simulations was 0.3 for both earlywood and latewood.

The FE model was constructed so that the angle θ of the rings could be changed (Fig. 8.4). The angles for the model were changes in 10° increments from 0 through 170°. Three different ring spacing were investigated (2, 4, or 6 rings per millimeter); three different proportions of latewood within each ring were investigated (1/2, 1/4, and 1/6 of the ring); and two locations (near the pith and near the bark) were investigated. The simulation test matrix investigated is given in Table 8.1. To this point we have run 210 FE simulations for Iosipescu specimens using the VFM to determine the displacement and strain fields.

8.3.3 *Grid Simulations*

A MATLAB® (MathWorks, Inc., Natick, MA USA) program has been developed to take FE displacements to create a synthetic displaced grid image. The grid simulation used the following assumptions for the grid and CCD camera: a grid pitch = 5 pixels with an array of 1360 pixels horizontally and 1024 vertically; a minimum grey level of 15 and a maximum

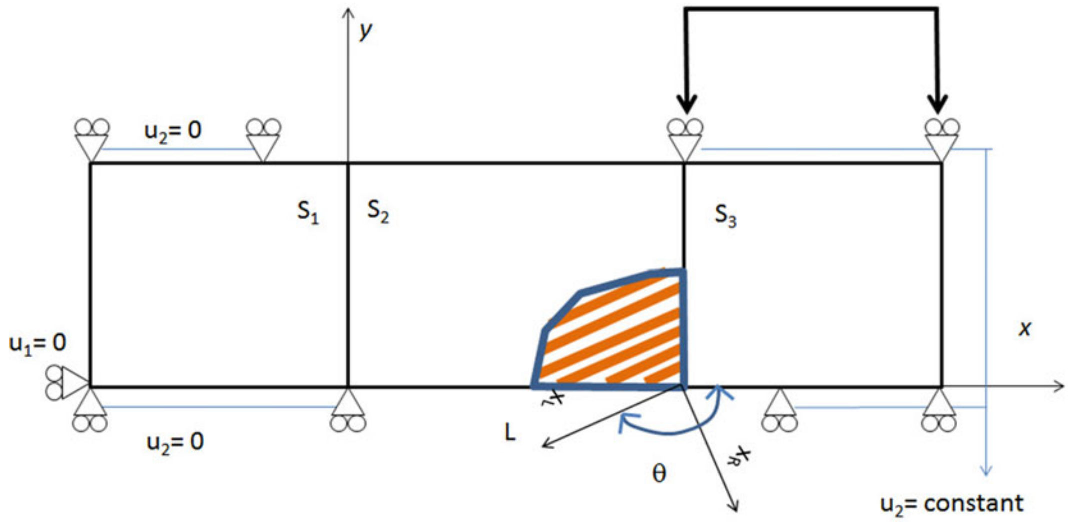

Fig. 8.4 Coordinates system for changing ring angle θ with respect to specimen coordinate system

Table 8.1 Simulation test matrix

		1/2 Ring width		1/4 Ring width		1/6 Ring width	
Ring space	2/1000	0–170	–	0–170	–	0–170	–
	4/1000	0–170	0–170	0–170	–	0–170	0–90
	6/1000	0–170	–	0–170	–	0–170	–

grey level of 4040, a pixel resampling of 5, and a minimum pitch for the grid of 0.1 mm. Figure 8.4 shows the comparisons between the FE strain maps and the simulated grid strain maps for a ring spacing of 2 rings per mm and 50 and 17 % latewood ring width for ring orientations of 0°, 40°, 60° and 90°. The first line of the figures are FE estimated ε_{xx} ε_{yy} and ε_{xy} values and the second line of the figure are grid simulated ε_{xx} ε_{yy} and ε_{xy} values. The strain maps for 40° and 60° orientations are quite similar for all ε values (Fig. 8.5).

8.4 Virtual Fields Method for Constitutive Parameter Identification

VFM for constitutive parameter identification is based on the principle of virtual work which can be written, in the case of plane stress and in the absence of body forces, and assuming a macroscopically homogeneous material with an orthotropic linear elastic behavior, as:

$$Q_{ij}\int_S \varepsilon_j \varepsilon_i^* dS = \frac{1}{t}\int_{S_f} T_\beta u_\beta^* dS \tag{8.1}$$

where Q_{ij} are stiffness parameters, ε_j are the actual strain components over S and, ε_i* is the virtual strain field associated with u_β*, S the surface of the interest of the plate, t the thickness of the plate, T_β the distribution of external tractions applied over S_f and u_β* the virtual displacement field.

with,

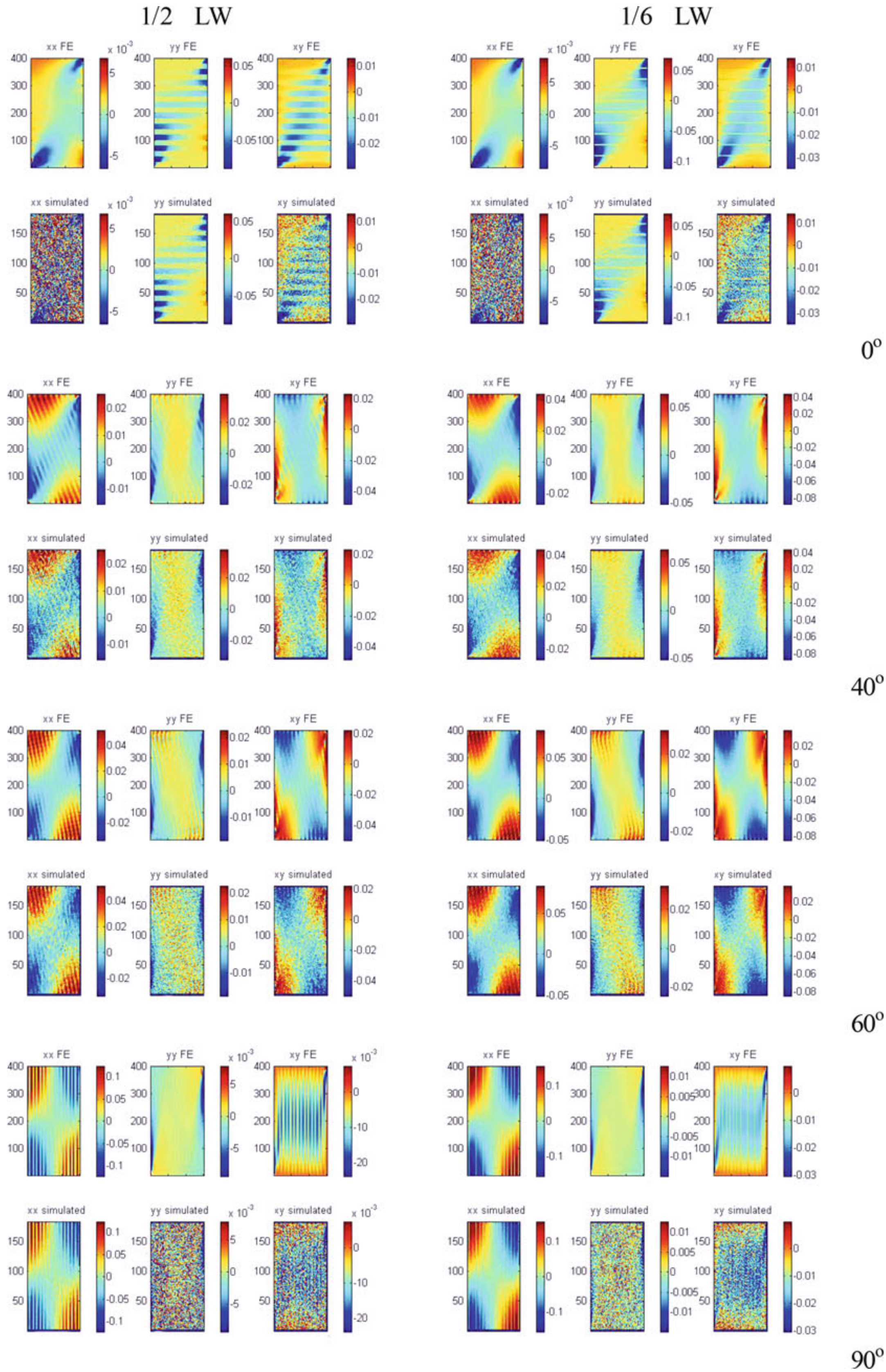

Fig. 8.5 Strains for FE and grid simulations for a ring spacing of 2 rings per mm and 50 and 17 % latewood ring widths at 0°, 40°, 60°, and 90°

$$Q_{ij} = \begin{bmatrix} Q_{11} & Q_{12} & 0 \\ Q_{12} & Q_{22} & 0 \\ 0 & 0 & Q_{66} \end{bmatrix} = \begin{bmatrix} \frac{E_{11}}{1 - v_{12}v_{21}} & \frac{-v_{21}E_{11}}{1 - v_{12}v_{21}} & 0 \\ \frac{-v_{12}E_{22}}{1 - v_{12}v_{21}} & \frac{E_{22}}{1 - v_{12}v_{21}} & 0 \\ 0 & 0 & G_{12} \end{bmatrix} \tag{8.2}$$

In (8.2) the symbols E, ν, and G represent, respectively, the modulus of elasticity, Poisson's ratio and the shear modulus and subscripts 1 and 2 denote the orthotropy axes. We have divided the measurement region, S, into earlywood and latewood (8.3).

$$Q_{ij}^{EW} \int_{S_{EW}} \varepsilon_j \varepsilon_i^* dS_{EW} + Q_{ij}^{LW} \int_{S_{LW}} \varepsilon_j \varepsilon_i^* dS_{LW} = \frac{1}{t} \int_{L_{S_2S_3}} T_\beta u_\beta^* dS \tag{8.3}$$

FE and grid simulation displacements and strains were used to determine the heterogeneous constitutive parameters using a VFM subroutine which had previously been programmed using Python programing language. The various Q values for earlywood and latewood based on FE and grid simulations were tabulated for comparison.

8.4.1 *Optimization of Angle Using Simulated Results*

The goal for conducting these simulations is determine the optimal ring orientation angle for testing specimens in the Iosipescu test fixture. Using the simulated experimental data, a parametric study investigated the effect of ring orientation as it varied between 0° and 180°. For the analysis reported below, we concentrated on the change between 0° and 90° because of expected symmetry. No random error is considered in this section, noise was not added to the synthetic grid image. This work will be addressed in future sensitivity studies. Error estimates were established for each stiffness estimate by comparing the stiffness parameters Q determined by FE models and the parameters Q determined by grid simulations using (8.4), where Q_{ijFEM} are the Qij results from the FE model and Q_{ijGrid} are the Qij results from the grid simulations.

$$E_{rr} = \frac{Q_{ijGrid} - Q_{ijFEM}}{Q_{ijFEM}} \tag{8.4}$$

An error function was introduced to evaluate the overall systematic error of the VFM identifications (8.5). This error function averages the amount individual error for the four most significant constitutive components 11, 22, 12, and 66. The components 16 and 26 were considered to be extremely small and not included in the function.

$$Error\_Function = \frac{1}{4}(|E_{11}| + |E_{22}| + |E_{12}| + |E_{66}|) \tag{8.5}$$

Figures 8.6 and 8.7 show the results for the range of ring spacing, proportion of ring width, and positions investigated to this point. Results for latewood are shown in red; results for earlywood are shown in black. The general shape of the error function for all variations tested appears to be similar. The error function is largest when away from angles between 30° and 60°. The largest values are for angles greater than 70°. The error function value has more variation as the proportion of latewood per ring increases. Also the most consistent minimum for the earlywood and latewood error function is between 40° and 50°. For the simulations that were conducted to look at the impact of changes in anisotropy (Fig. 8.7, the stiffness of LW was cut in half), there appears to be little impact on the shape of the error function. A summary of the angles with the

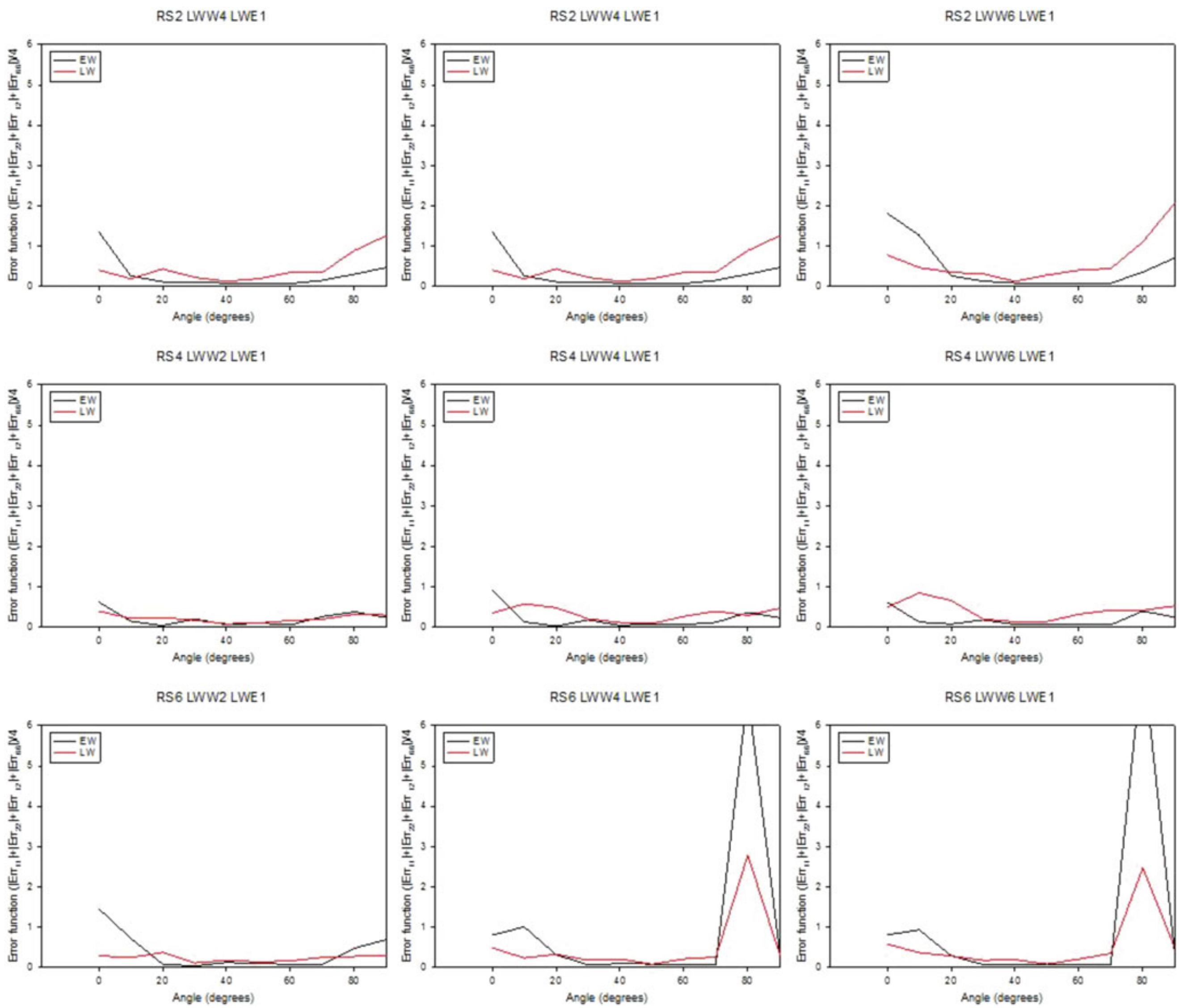

Fig. 8.6 Earlywood and latewood error functions for nine combinations of ring spacing and latewood width [RS is ring spacing (2, 4, or 6 rings per mm), LWW is latewood width (1/2, 1/4, or 1/6), LWE indicates if latewood stiffness values are (near bark 1 or near pith 0.5)]

lowest error functions for the different configurations explored is given in Table 8.2. Results so far would suggest that a starting angle of 45° would be an effective ring orientation for the un-notched Iosipescu test specimen.

8.5 Summary

A series of finite element (FE) and grid simulations were conducted to determine displacement and strain fields for various ring angles, ring spaces, and proportion of latewood per ring. These displacement and strain fields were utilized to determine the constitutive information for the woody material using the VFM. Using an error function based on a comparison of the FE and grid simulation constitutive parameters, it was possible to select the ring angle at which test specimens should be tested for best Q_{ij} identification. The results of this work suggest that 45° ring orientation gives lowest errors for the un-notched Iosipescu test geometry.

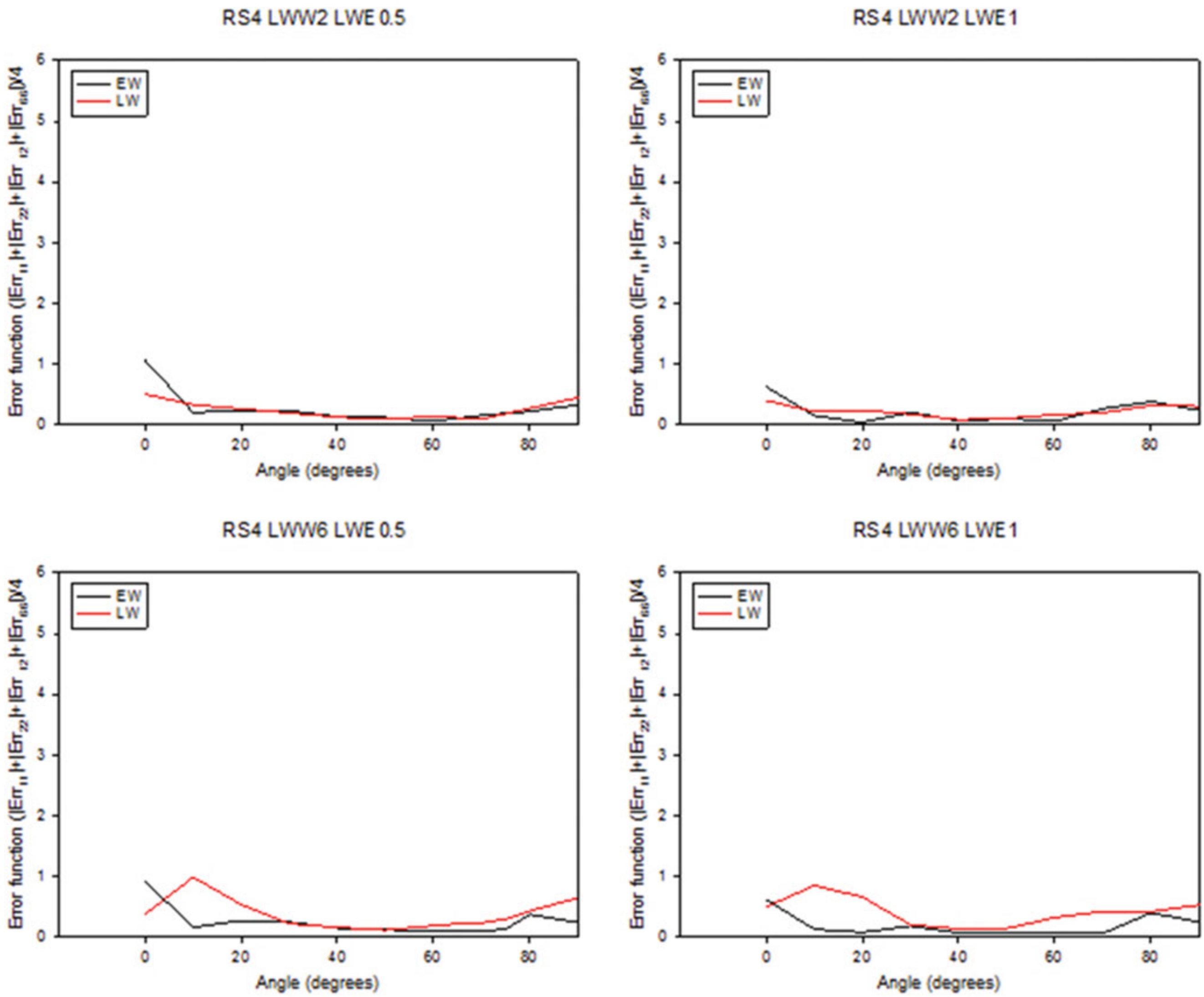

Fig. 8.7 Error function results for pith and bark anisotropy ratios [RS is ring spacing (4 rings per mm), LWW is Latewood width (1/2, or 1/6 of ring), LWE indicates if latewood stiffness values are (near bark 1 or near pith 0.5)]

Table 8.2 Ring angles with the lowest cost functions

		1/2 Ring width		1/4 Ring width		1/6 Ring width	
		Near bark	Near pith	Near bark	Near pith	Near bark	Near pith
Ring space	2/1000	40	–	40	–	40	–
	4/1000	40–50	40–60	40–50	–	40–50	40–50
	6/1000	30–50	–	50	–	50	–

8.6 Future Plans

There will be a continuation of exploring the random and systematic errors of this measurement technique. A series of experimental tests using un-notched Iosipescu test fixture (Fig. 8.2) will begin in the spring of 2015. The initial testing will be conducted on Loblolly pine and then progress on to Lodgepole pine.

References

1. P.R. Larson, D.E. Kretschmann, A. Clark III, J.G. Isebrands, Juvenile wood formation and properties in southern pine. *General Technical Report, FPL GTR 129*, U.S. Department of Agriculture, Forest Service, Forest Products Laboratory, Madison, 2001, p. 42
2. M. Grediac, F. Pierron, S. Avril, E. Toussaint, The virtual fields method for extracting constitutive parameters from full-field measurements: a review. Strain **42**, 233–253 (2006)
3. J. Xavier, S. Avril, F. Pierron, J. Morais, Novel experimental approach for longitudinal-radial stiffness characterization of clear wood by a single test. Holzforschung **61**(5), 573–581 (2007)
4. J. Xavier, S. Avril, F. Pierron, J. Morais, Variation of transverse and shear stiffness properties of wood in a tree. Compos. Part A **40**(12), 1953–1960 (2009)
5. S.M. Cramer, D.E. Kretschmann, R. Lakes, T. Schmidt, Earlywood and latewood elastic properties in loblolly pine. Holzforschung **59**(5), 531–538 (2005)
6. D.E. Kretschmann, S.M. Cramer, The role of earlywood and latewood properties on dimensional stability of wood. Chapter. *The Compromised Wood Workshop 2007*, University of Canterbury, Christchurch, 29–31 January 2007, pp. 215–236
7. D.E. Kretschmann, The influence of juvenile wood content on shear parallel compression and tension perpendicular to grain strength and mode I fracture toughness of loblolly pine at various ring orientations. For. Prod. J. **58**(7/8), 89–96 (2008)
8. T.M. Gorman, D.E. Kretschmann, Characterization of juvenile wood in Lodgepole pine in the intermountain west. In: *Proceedings of the 55th International Convention of Society of Wood Science and Technology*, Beijing, 27–31 August 2012
9. F. Pierron, The virtual fields method, extracting constitutive mechanical parameters from full-field deformation measurements short course. In: *16th International Conference on Experimental Mechanics, ICEM 16*, Cambridge, 6 July 2014
10. Y. Surrel, Fringe Analysis, in *Photomechanics*, ed. by P. Rastogi. Topics in Applied Physics (Springer, Heidelberg, 1999), pp. 57–104
11. M. Rossi, F. Pierron, On the use of simulated experiments in designing tests for material characterization from full-field measurements. Int. J. Solids Struct. **49**(3–4), 420–435 (2012)